



Laboratori Nazionali di Frascati

LNF-88/11(P)

18 Febbraio 1988

G. Pancheri and Y.N. Srivastava:

NON SCALING PHENOMENA IN LOW- p_t PHYSICS

Contributed Talk to the
Shandong Workshop on Multiparticle Production
Jinan, China, June 28 - July 6 (1987)

Servizio Documentazione
dei Laboratori Nazionali di Frascati
P.O. Box, 13 - 00044 Frascati (Italy)

INFN - Laboratori Nazionali di Frascati

Servizio Documentazione

LNF-88/11(P)

18 Febbraio 1988

Non-scaling Phenomena in low- p_t physics

Giulia Pancheri

INFN, Laboratori Nazionali di Frascati, P.O.Box 13, 00044 Frascati, Italy
High Energy Physics Laboratory, Harvard University, Cambridge, Massachusetts 02138

and

Yogendra N.Srivastava

INFN, Dipartimento di Fisica, Università' di Perugia, 06100 Perugia, Italy
Physics Department, Northeastern University, Boston, Massachusetts 02115

Following the Shandong workshop spirit, in this paper we shall try to summarize the work we have been doing in this field in the last few years. From the beginning, our interest was to understand some of the large cross-section features using QCD calculations and techniques. In our first approach to the field, we suggested that the characteristic shape of the KNO function ^[1] could be explained by applying soft gluon summation formulae ^[2] to particle emission processes. These techniques and the expression we thus obtained for the KNO distribution are described in section 1 of this note. In our model the shape of the KNO function depended upon a parameter β , the single soft gluon spectrum averaged over the hadronic matter coordinates at any given energy. While the strength of our approach was that it was possible to find a value of β which could reproduce the KNO function at various energies or rapidity intervals, we also found that the energy behaviour of this parameter was contrary to its naive QCD interpretation. We were thus led to the hypothesis that KNO scaling violations ^[3,4] could arise from a two component type behaviour, with a soft part responsible for the low energy shape and a "new" energy dependent part, which

we labelled as a hard component, and which we attributed to the emergence of hard gluon scattering at CERN Collider energies, $\sqrt{s} \approx 100 \div 900 \text{ GeV}$. According to this hypothesis^[5], many other non-scaling phenomena in this energy region should be explained as due to the emergence of hard gluon-gluon scattering. A still incomplete list of some of these low- p_t scaling violations include :

- (i) rise of the plateau^[6], i.e. violation of Feynman scaling whereupon one observes a logarithmic increase with energy in the number of particles produced at 90 deg ;
- (ii) a faster than logarithmic increase in the average multiplicity ;
- (iii) KNO scaling violations, implied by the two previous non-scaling behaviours ;
- (iv) a logarithmic increase in the ratio of strange to non-strange particles ;
- (v) a flattening with energy^[6] of the single particle p_t distribution, with $\langle p_t \rangle$ higher in high multiplicity events, an effect which becomes more pronounced as the energy increases^[7].
- (vi) a faster than logarithmic increase in the total inelastic cross-section^[8].

The two component model^[9], which we sketch in section 2, required an unexpectedly large fraction of hard gluon-gluon scattering events, of the order of 10 \div 20% relative to the soft part. With such a simple model one could understand not only the widening of the KNO distribution but also the increase of $\langle p_t \rangle$ with multiplicity. While the two component model is certainly not complete past our present energy range, since it can only be justified up to a first order QCD calculation, it had the virtue of pointing to the presence of a large contribution from hard gluon-gluon scattering. A QCD calculation of this contribution is discussed in section 3. The presence of a large gluon-gluon scattering contribution was indeed found by the UA1 collaboration, through the so-called mini-jet analysis^[10]. While some of the gross features of the mini-jet sample (KNO distribution for instance) can also be understood in terms of a statistical analysis like the one by Meng-Ta Chung and his collaborators^[11], the UA1 work shows that the jets from the mini-jet sample, in terms of angular and transverse momentum distribution, satisfy the same requirements of the high- p_t jet sample^[12]. The interpretation of these events in terms of hard scattering is thus experimentally justified. The question now arises as to how to go beyond the two component model, which as we said, cannot be complete in its present form. From a phenomenological point of view, this model gives higher energy predictions for the KNO function which are not borne out by other models^[13]. In particular the two component model in the form we had suggested does not predict a further widening of the KNO distribution. This may not be correct. At present there are a variety of models which incorporate the two component structure in the eikonal function for the total cross section. In section 4 we shall briefly mention the work done along these lines together with our assessment of these efforts. A hindrance to the predictive power of these models is that one has to assume the impact parameter space distribution of partons within the hadrons.

1. Soft Gluon Bremsstrahlung and KNO Distribution

The problem of understanding the shape of the hadronic multiplicity distribution and of its approximate scaling in the KNO variable, $z = \frac{n}{\langle n \rangle}$, still represents an outstanding question in strong interaction physics. In 1972 Koba, Nielsen and Olesen predicted on the basis of Feynman scaling and the approximate logarithmic growth of the mean multiplicity, $\langle n(s) \rangle \approx \ln s$, that the function

$$\Psi(z, s) = \langle n \rangle \frac{\sigma_n(s)}{\sum_n \sigma_n}$$

should remain constant with changes in energy. In the soft QCD bremsstrahlung model^[2], the shape of the KNO function is obtained from that of the soft QCD radiation emitted in the scattering of quarks and gluons. By summing all soft massless quanta emitted in the collision one obtains the following expression for the energy distribution of the emitted radiation :

$$\frac{dP}{d\omega} = \int \left(\frac{dt}{2\pi} \right) e^{i\omega t - h(E, t)} \quad (1)$$

where

$$h(E, t) = \int_0^E \left(\frac{d^3k}{2k} \right) |j_\mu(k)|^2 (1 - e^{-ikt}) \quad (2)$$

and

$$|j_\mu(k)|^2 = \frac{2\alpha_s(k_\perp)}{\pi^2 k_\perp^2}$$

The parameter \bar{E} represents the maximum energy which a single soft gluon can carry away in a given parton-parton collision. Assuming that on the average the final state pions equally share the radiated energy, we made the substitution

$$\omega = n \langle \text{energy} \rangle_{\text{single pion}}$$

so as to obtain for the KNO function the expression

$$\Psi\left(\frac{n}{\langle n \rangle}\right) = \beta(s) \int \frac{dt}{2\pi} e^{iz\beta(s)t - \beta(s) \int_0^1 \frac{dk}{k} (1 - e^{-ikt})} \quad (3)$$

The parameter $\beta(s)$ which appears in the above expression is an effective soft gluon spectrum which incorporates the averaging process which takes place when eq.(1) is integrated between initial parton densities and final hadron fragmentation. To wit, we have written

$$\langle dP(\omega, E) \rangle = d \left\langle \frac{\omega}{E} \right\rangle \int \frac{dt}{2\pi} e^{i \left\langle \frac{\omega}{E} \right\rangle t - \langle h(t) \rangle} \quad (4a)$$

with

$$\langle h(t) \rangle = \beta(s) \int_0^1 \frac{dk}{k} (1 - e^{-ikt}) \quad (4b)$$

and the symbol $\langle \rangle$ indicates the above mentioned average. We expect the effective parameter $\beta(s)$ to have a residual $\ln \ln s$ dependence as well as to be proportional to the color factors $c_F (= \frac{4}{3})$ or $c_A (= 3)$ according as to whether the emitting partons were quarks or gluons. The bremsstrahlung distribution of eq.(3) cannot be obtained in closed form for general values of the ratio $\langle \frac{\omega}{E} \rangle$. To evidentiate the small and large z behaviour of the function Ψ , it is convenient to approximate eq.(4b) as follows :

$$\langle h(t) \rangle \approx b \log[1 + it]$$

which, after some simple manipulations, leads to

$$\Psi(z) \approx \frac{b}{\Gamma(b)} (bz)^{b-1} e^{-bz} \quad (5)$$

A numerical comparison between eqs.(3) and (5) shows that the two distributions have the same shape for $b \approx 2\beta(s)$. Eq.(5) is one of the limits of the negative binomial distribution, introduced originally by Giovannini^[14] and later by Carruthers and Shih^[15] to describe the multiplicity distribution and widely used, at present, to fit the KNO function in various rapidity intervals and in various processes.

The shape of the KNO function is completely determined by the spectrum β . Thus, if we treat β as a parameter, we can obtain the shape at lower energies and, changing β , at higher energies. Let the moments of the KNO function be defined as

$$C_k = \langle z^k \rangle = \int z^k \Psi(z, s) dz$$

then, the following expressions can be easily obtained, through successive partial integrations, from eq.(3) :

$$\langle z^2 \rangle = 1 + \frac{1}{2\beta} \quad (6a)$$

$$\langle z^3 \rangle = 1 + \frac{3}{2\beta} + \frac{1}{3\beta^2} \quad (6b)$$

$$\langle z^4 \rangle = 1 + \frac{3}{\beta} + \frac{25}{12\beta^2} + \frac{1}{4\beta^3} \quad (6c)$$

$$\langle z^5 \rangle = 1 + \frac{5}{\beta} + \frac{95}{12\beta^2} + \frac{35}{12\beta^3} + \frac{1}{5\beta^4} \quad (6d)$$

Fixing the value of β from C_2 , we obtain the values shown in Table I for the moments at lower energy, i.e. up to $\sqrt{s} = 63 GeV$, and in Table II for the moments at higher energies, i.e. at the Cern proton-antiproton collider.

TABLE I. $\sqrt{s} = 63\text{GeV}$

1 Component Model

C_k	Model Predictions	ISR Data ^[16]
C_2	1.2 (fixed)	1.2 ± 0.01
C_3	1.653	1.67 ± 0.03
C_4	2.55	2.63 ± 0.09
C_5	4.46	4.6 ± 0.2

The theoretical values are obtained from eq.(6a), fixing $C_2 = 1.2$ ($\beta = 2.5$).

TABLE II. $\sqrt{s} = 540\text{GeV}$

1 Component Model

C_k	Model Predictions	UA5 Data ^[3]
C_2	1.31 (fixed)	$1.31 \pm 0.01 \pm 0.03$
C_3	2.06	$2.12 \pm 0.03 \pm 0.11$
C_4	3.73	$4.05 \pm 0.10 \pm 0.30$
C_5	7.89	$8.8 \pm 0.4 \pm 0.9$

Theoretical values are obtained from eq.(6) fixing $C_2=1.31$ ($\beta = 1.62$).

The agreement between the experimental and the theoretical values for C_3, C_4 and C_5 points to the validity of the description of the multiplicity distribution in terms of a fourier transform of an exponentiated bremsstrahlung spectrum of the type $\beta \frac{dk}{k}$. At the same time, we notice that the rise in the higher moments from ISR to Collider energies is quantitatively accounted for with a decrease in the effective β from $\beta_{ISR} = 2.5$ to $\beta_{collider} = 1.62$. The soft gluon model exposed in ref.[2], does not explain a decrease in the effective gluon spectrum. If there were no new production mechanisms between lower energies and the collider, β should grow, albeit slowly, $\approx \ln \ln s$. Thus a decrease in the effective β must signal some new production mechanism (jets, mini-jets, multipartons, etc.) with a threshold around the ISR energy.

2. The Two Component Model

It appears that at large multiplicities, $n \simeq 2 \div 3 < n >$, there is an excess of events over the asymptotic KNO fit at lower energies. Although the fraction of 'abnormal' events is relatively small, the effect is very conspicuous when the higher moments of the KNO function are compared at different energies. Up to ISR energies, the moments are approximately constant^[16,17], thus indicating that the shape of the curve does not change, i.e. that KNO scaling holds. However after the ISR energies, the higher moments, which

are more sensitive to the larger multiplicity region, drastically change. This might indicate a new production mechanism which becomes significant at CERN collider energies and which is characterized by a higher mean multiplicity. We have suggested that the new mechanism is related to the appearance of gluon initiated processes, which were quite negligible in the ISR range but which start showing up at the collider, most noticeably in jet production. Indeed, there are three observations, concerning jet production, which are relevant to this discussion : (i) at the Cern Collider the energy is high enough to allow for hard scattering between many low-x partons, leading to the production of mini-jets, i.e. jets around and below the lowest detectable threshold, (ii) at low x the dominant QCD subprocess in jet production is gluon-gluon scattering, (iii) the UA1 collaboration has reported that the multiplicity of the background accompanying the jets, what has been called the "jet floor" in a multiplicity vs. rapidity plot, is more than twice the minimum bias multiplicity and is independent of the transverse energy of the trigger jet, remaining high ($\simeq 2 < n(s) >$) down to rather low values of the trigger^[12]. The new production mechanism, as far as the multiplicity is concerned, can be conceivably related to a strong increase in the number of events associated with hard gluon-gluon scattering. Let us now show how a two component model^[18] can account for KNO scaling violations as well as the flattening of inclusive single particle spectra.

The simplest way to verify phenomenologically the above hypothesis is to separate the cross-section in two parts, such that

$$\sigma(s) \approx \sigma_0(s) + \sigma_1(s) \quad (7)$$

$$\frac{d\sigma}{dn} \approx \frac{d\sigma_0}{dn} + \frac{d\sigma_1}{dn} \quad (8)$$

$$\frac{d\sigma}{dn dp_t} \approx \left(\frac{d\sigma_0}{dn} \right) \frac{dP_0(p_t)}{dp_t} + \left(\frac{d\sigma_1}{dn} \right) \frac{dP_1(p_t)}{dp_t} \quad (9)$$

where the first and second term on the right hand side represent respectively the dominant low energy multiparton cross section and its first order α_s correction due to hard parton-parton scattering. dP_0 and dP_1 are normalized probabilities describing the p_t -distribution of single pions. For simplicity, we shall denote the two components as non-perturbative and perturbative. For the first term, KNO scaling holds well and the transverse momentum distributions show no dependence upon the multiplicity. While eq.(9) is an improvement over the naive expectation

$$\frac{d\sigma}{dn dp_t} \approx \frac{d\sigma}{dn} \frac{dP}{dp_t}$$

it is still a gross approximation since the perturbative term, at least, receives contributions from processes which may be quite different from the point of view of particle production like quark-quark, quark-gluon and gluon-gluon scattering. Integrating eq.(9), one obtains

$$\langle p_t \rangle = \frac{\langle p_t \rangle_0 \frac{d\sigma_0}{dn} + \langle p_t \rangle_1 \frac{d\sigma_1}{dn}}{\frac{d\sigma_0}{dn} + \frac{d\sigma_1}{dn}}$$

where $\langle p_t \rangle_0$ and $\langle p_t \rangle_1$ refer to particles emitted in the non-perturbative and perturbative processes respectively.

At the same time, from eq.(8), we get the KNO distribution of the entire sample in terms of those of the two components, i.e. :

$$P_n(s) = \frac{\sigma_n}{\sum_n \sigma_n} = \frac{1}{\langle n \rangle} \frac{\Phi_0\left(\frac{n}{\langle n \rangle_0}\right) + r \Phi_1\left(\frac{n}{\langle n \rangle_1}\right)}{1 + r} \quad (10)$$

so that

$$\langle p_t \rangle = \frac{\langle p_t \rangle_0 \Phi_0\left(\frac{n}{\langle n \rangle_0}\right) + r \langle p_t \rangle_1 \Phi_1\left(\frac{n}{\langle n \rangle_1}\right)}{\Phi_0\left(\frac{n}{\langle n \rangle_0}\right) + r \Phi_1\left(\frac{n}{\langle n \rangle_1}\right)} \quad (11)$$

with

$$r = \frac{\sigma_1}{\sigma_0}$$

and

$$\Phi_i(z_i) = \langle n \rangle \frac{1}{\sigma_i} \frac{d\sigma_i}{dn} = \frac{\langle n \rangle}{\langle n \rangle_i} \Psi(z_i)$$

where Ψ_0 and Ψ_1 are the KNO functions of the two terms and $z_i = \frac{n}{\langle n \rangle_i}$. In the above equations, $r = \frac{\sigma_1}{\sigma_0}$ represents the fraction of jetty events over the non-jetty ones. As we discuss in section 3, the contribution σ_1 , which can be calculated perturbatively, strongly depends upon the minimum cut-off in the jet transverse momentum.

Eq.(11) now shows that if Φ_1 is characterized by an average multiplicity $\langle n \rangle_1$ substantially larger than that of Φ_0 , the influence of the second term becomes important at large n . Thus $\langle p_t \rangle$ would slowly grow and reach its maximum at $n \approx \langle n \rangle_1$. In this simple formulation, the energy dependence of $\langle p_t \rangle$ and $\langle n \rangle$ comes from the ratio $r(s)$. Integrating eqs.(8) and (9) over n one easily sees that $\langle p_t \rangle$ is a linearly growing function of $\langle n \rangle$. This is approximately verified by the data, as shown in Fig.1.

A two component model easily accounts also for the observed violations of KNO scaling. This can be shown using the soft QCD radiation model discussed in the previous section for the KNO functions needed in eqs.(10) and (11). Previously [2], we had obtained

$$\Psi\left(\frac{n}{\langle n \rangle}\right) = \beta \int \frac{dt}{2\pi} \exp\left(i\beta \frac{n}{\langle n \rangle} t - \beta \int_0^1 \frac{dk}{k} (1 - e^{-ikt})\right)$$

by assuming that the energy carried by the n -particles observed in the final state was shed off as radiation during the hadronic collision. The parameter β is a measure on the average of the exponentiated soft gluon spectrum. Thus β is proportional to the strong coupling

Mean Transverse Momentum vs. Multiplicity

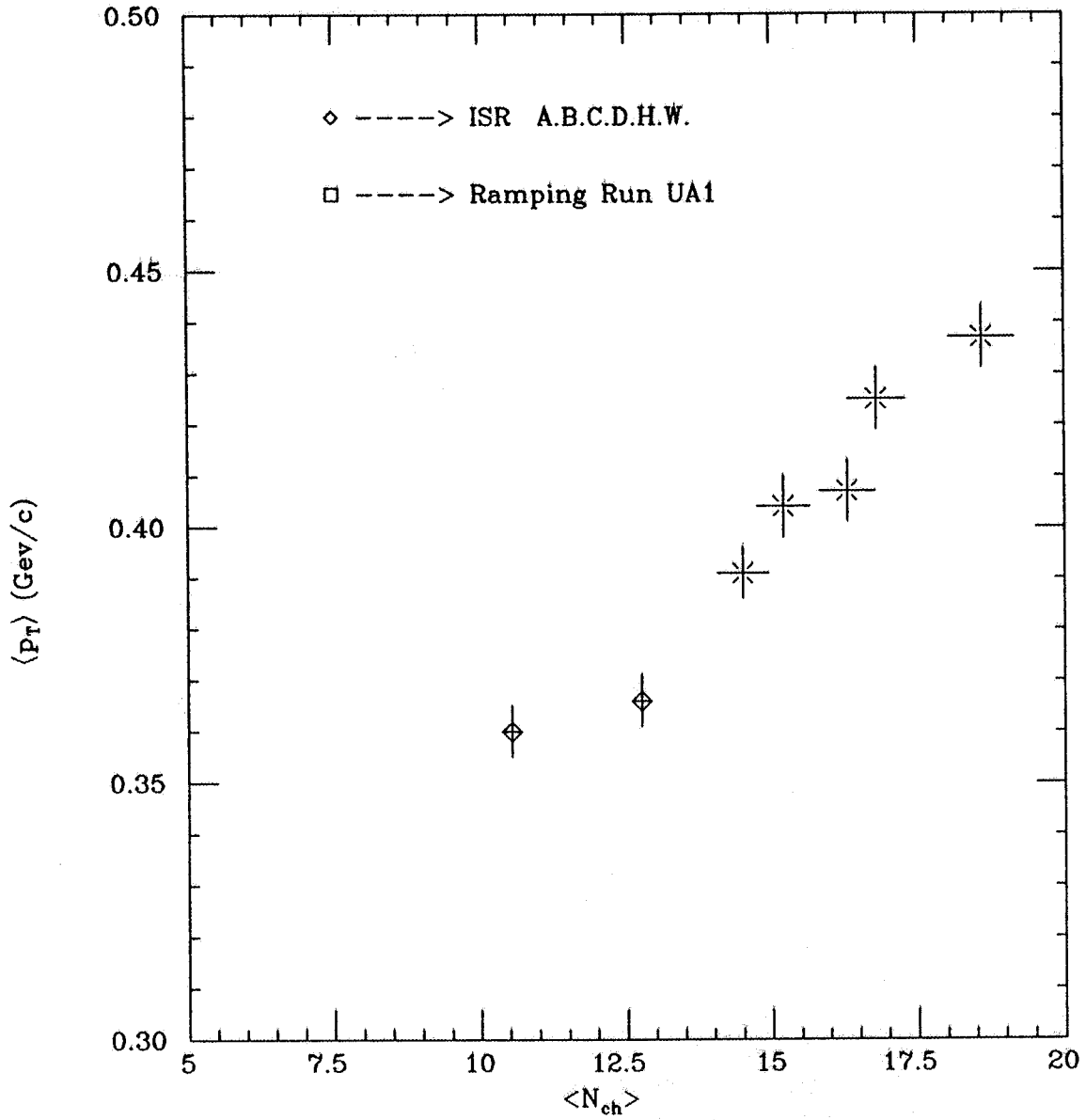


Fig. 1 The measured average transverse momentum per single particle is shown as a function of the average multiplicity at the same center of mass energy. Data are from ref. 7 for the ISR data and from refs.(10)and (12) for the CERN Collider.

constant α_s and to the color factors characteristic of the underlying process. Referring to radiation from a gluon or radiation from a quark, one has

$$\frac{\beta_{gluon}}{\beta_{quark}} \approx \frac{c_A}{c_F} = \frac{9}{4}$$

as well as

$$\frac{\langle n_{gluon} \rangle}{\langle n_{quark} \rangle} \approx \frac{c_A}{c_F}$$

We assume that the first (non-perturbative) component proceeds mostly through quark radiation. On the other hand, at high energy (CERN Collider and beyond) radiation and fragmentation from hard parton-parton scattering (second component) should appear as a non-negligible fraction of the cross-section, and be dominated by gluon-gluon scattering.

From eq.(8), we obtain

$$\langle n(s) \rangle = \frac{\langle n_0(s) \rangle + r(s) \langle n_1(s) \rangle}{1 + r(s)} \quad (12)$$

where, according to the previous discussion,

$$\frac{\langle n_1(s) \rangle}{\langle n_0(s) \rangle} \approx \frac{c_A}{c_F} \approx \frac{\beta_1}{\beta_0} \quad (13)$$

Making use of eq.(13), we can rewrite eq.(10), as follows :

$$\Psi(z, s) = \beta \int_{-\infty}^{\infty} \frac{d\tau}{2\pi} e^{i\beta z \tau} \frac{1}{1+r} \left(e^{-\beta_0 \int_0^1 \frac{dk}{k} (1-e^{-ik\tau})} + r(s) e^{-\beta_1 \int_0^1 \frac{dk}{k} (1-e^{-ik\tau})} \right)$$

with

$$\frac{\beta}{\langle n \rangle} \approx \frac{\beta_0}{\langle n_0 \rangle} \approx \frac{\beta_1}{\langle n_1 \rangle}$$

We now turn to compute C_k for the two component model. The results are shown in Table III.

TABLE III
Two-Component Model, $r=0.12$

C_k	Model Predictions	UA5 Data ^[3]
C_2	1.275	$1.31 \pm 0.01 \pm 0.03$
C_3	2.014	$2.12 \pm 0.03 \pm 0.11$
C_4	3.822	$4.05 \pm 0.10 \pm 0.30$
C_5	8.524	$8.8 \pm 0.4 \pm 0.9$

To obtain the values shown in the above table, we have scaled β_0 according to the asymptotic freedom formula

$$\beta_0(\sqrt{s} = 540 \text{ GeV}) = \beta_0(\sqrt{s} = 63 \text{ GeV}) \frac{\ln \ln \left(\frac{540}{\Lambda} \right)^2}{\ln \ln \left(\frac{63}{\Lambda} \right)^2} \simeq 2.78$$

and have used the approximate relation given by eq.(13), and set $\Lambda = 100 \text{ MeV}$. The table shows that this two component model can quantitatively account for the observed scaling violations in the collider region.

Using the above parameters, $\beta_0 = 2.78$, $\beta_1 = \frac{9}{4}\beta_0$ and $r=0.12$, we show in Fig.2 a plot of $2\Psi(z)$ vs. z and its comparison with the recent UA5 data.

To predict the shape of the KNO function for even higher energies (Tevatron, LHC, SSC, ...) we need to specify the energy dependence of $r(s)$ in eq.(13). We parametrize

$$r(s) = \alpha_1 + \alpha_2 \ln s \quad (14)$$

and choose $\alpha_{1,2}$ as follows. At FNAL energies ($\sqrt{s} \leq 28 \text{ GeV}$) as well as at ISR around $\sqrt{s} \approx 30 \text{ GeV}$, KNO scaling holds reasonably well. Thus we set $r(30 \text{ GeV})=0$. The leftover parameter is then determined by fixing $r(540 \text{ GeV})=0.12$ as above. As a check we have computed $r(s)$ using eq.(14) at $\sqrt{s} = 63 \text{ GeV}$, the highest ISR energy. We find $r(63 \text{ GeV})=0.03$, indeed small to justify a posteriori our earlier neglect of σ_1 , up to highest ISR energies. Our predictions for the KNO function at $\sqrt{s} > 1 \text{ TeV}$ however show the model limitations. Indeed, as one can easily see by taking the high energy limit of eq.(13), when $r(s)$ become larger than 1 the second component starts taking over from the first until, at the end, the distribution simply shifts from the first component to the second component. This precludes any further widening of the distribution. Is this what we really expect at SSC energies and beyond ? To answer this question one must try to put the two component model in a theoretical framework and try to understand and to compute the relative fraction of events coming from the two different components. We shall try to answer this question in the next section.

3. QCD Calculation of low - p_t jet yield

A high energy hadron-hadron collision is an extremely complicated, simultaneous interaction between a very large number of different energy partons participating to the event. Therefore, in addition to hard parton- parton scattering, there are additional processes which take place simultaneously and which produce particles associated with the so called *underlying event*. Note that the structure of the underlying event may be affected by the dynamics of the hard scattering. Notwithstanding these difficulties, as a first step, one can try to separate σ_{tot} into two terms, $\sigma_{tot} \approx \sigma^{NP} + \sigma^{QCD}$ where the first term contains non-perturbative contributions, while the second receives contributions from processes which can be satisfactorily described by perturbative QCD.

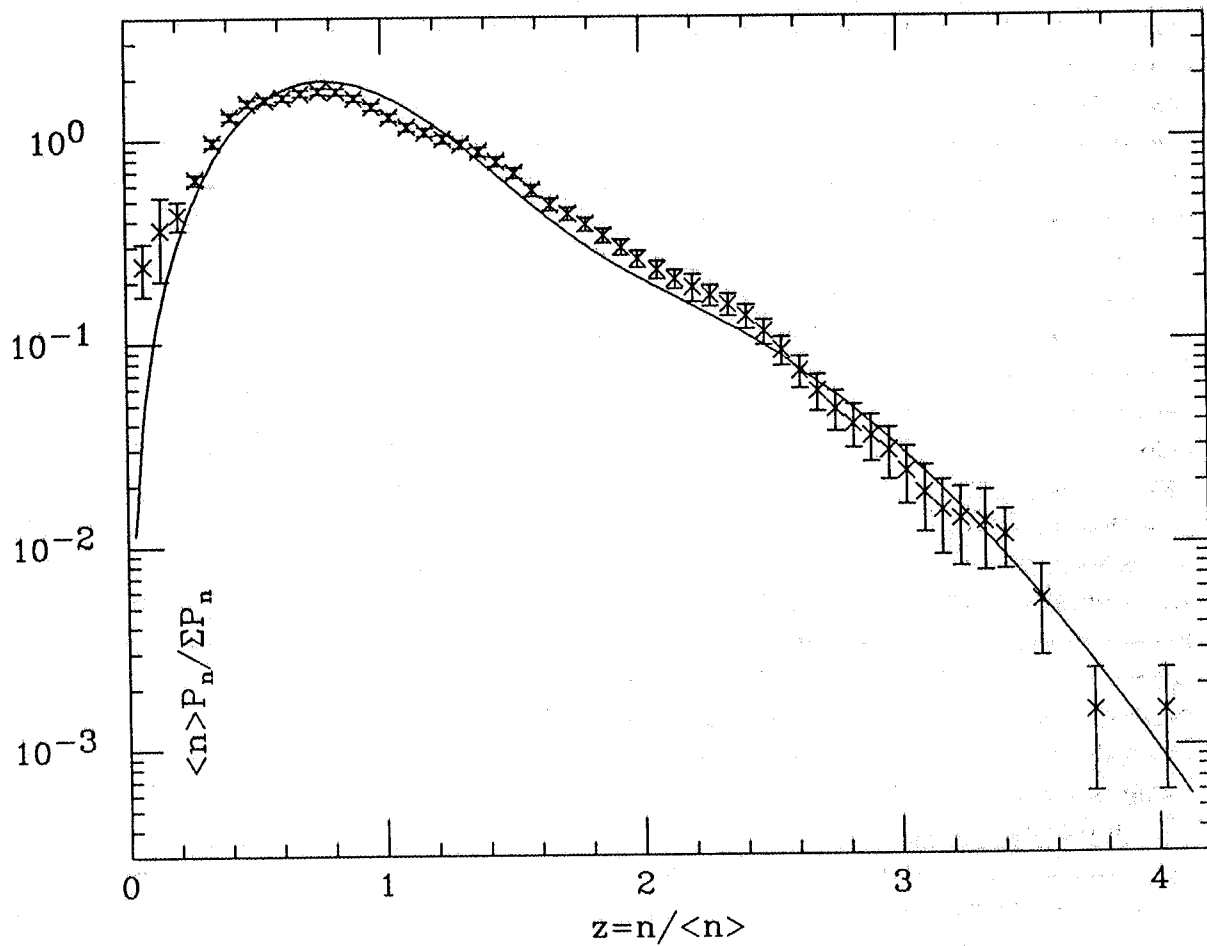


Fig.2 The KNO function from UA5 data, ref. 3, is compared with the theoretical curve from the two component bremsstrahlung model of ref. 9.

Perturbative QCD is in many ways indivisibly related to the experimental observation of jets . In order to establish a $\sigma^{(QCD)}$ which could give a significant contribution to σ_{tot} the observable jet phenomenon must be greatly enhanced (many orders of magnitude) and extended to transverse energies E_T which are much smaller than those reported by the already classic experiments at the CERN Collider . In this section we shall examine the possibility that σ^{QCD} may be an important fast rising part of σ_{tot} already at the CERN Collider. Indeed it is possible that if not the totality ,at least a major fraction of the rise of σ_{tot} -which from $\approx 39\text{mb}$ at $\sqrt{s} = 22\text{GeV}$ is now $\approx 60\text{mb}$ at $\sqrt{s} = 630\text{ GeV}$ [8] (and it is commonly presumed to reach even larger values at very high energies from cosmic rays [19]) can be related to the hypothesis that low-energy jets are responsible for KNO and other scaling violations. To make this connection viable, it is necessary that the fraction of jetty events becomes as much as $10 \div 20\%$ of the inelastic cross-section and grow with energy from the very small value recorded at the ISR. It is then predicted that the jet phenomenon at the collider will become a significant fraction of all events rather than a very specialized effect with tiny cross-section. This can be formally achieved since the lowest order cross-section becomes arbitrarily large if extended to lower and lower p_t values. Therefore there must be a minimum transverse momentum p_{cut} above which perturbative QCD can be safely applied. The value of such a parameter is related to the experimental jet resolution threshold and it is expected to be a slowly varying function of the collider energy. Note that this cut-off may be lower than the energy at which jets are still experimentally observable, since the detection of low energy "jets" in a hadronic background coming from the underlying event is not easy and it may depend on its choice of definition.

The UA1 collaboration [10,12] has reported the direct observation of such low- E_T jets. It becomes therefore possible to have a direct experimental clue about how large can $\sigma^{(QCD)}$ be and on the value of the lowest transverse momentum cut-off p_{cut} . Indeed the experimental data provide the right amount of jet cross-section to explain KNO scaling violations and the increase of $\langle p_t \rangle$ with multiplicity according to the two component model, at the same time we shall show that they can be well understood in terms of simple QCD calculations accounting for as much as $\approx 20\%$ of the total inelastic cross-section.

If such low-x parton parton collisions become relevant it is eventually necessary to take into account also cases in which multiple, independent parton scattering become observable in the same event. At yet higher energies this phenomenon is expected to play a non-negligible role and must be included in the estimate of $\sigma^{(QCD)}$.

For very large transverse energies the jet phenomenon is rather striking. Its kinematics is well understood by QCD predictions, as reflected in the two-jet angular distribution [20]. Cross-sections are well described by QCD calculations and structure functions which are extrapolated in Q^2 from neutrino scattering data. In these calculations the energy range is artificially limited by the experimental cuts to a domain in which a number of approximations are valid and which is very far from the minimum transverse momentum p_{cut} above which perturbative QCD can be applied.

As discussed in these proceedings [21] the UA1 collaboration has recently reported the observation of inclusive jet production down to transverse energies of a few GeV, at

$\sqrt{s} = 540 \text{ GeV}$ and 630 GeV and through the energy range $\sqrt{s} = 200 \div 900 \text{ GeV}$ ¹⁰⁾. These events have typical energies of the jets once recorded at the ISR and E_T as much as ten times smaller than the jets previously reported at the collider. Therefore they are more difficult to study experimentally. With these measurements the differential jet cross-section now spans an interval of almost 10 orders of magnitude, from $\approx 1 \text{ mb}$ at $E_T = 5 \text{ GeV}$ down to less than 10^{-9} mb at $E_T \approx 150 \text{ GeV}$. New problems also arise in comparing these results with theory since it is not known how low in E_T one can go before perturbative QCD becomes too rough an approximation and because differences in the choice of scale are more evident in the low- E_T region.

The following remarks about the minimum bias jet cross-section can be made :

- (i) the distribution of minimum bias jets appears to join in smoothly with that at high E_T from the jet trigger ;
- (ii) the agreement with the QCD curve is reasonable, and within the various uncertainties discussed previously ,
- (iii) the newly measured UA1 jet cross-section from minimum bias follows the general behaviour of the high- E_T jets and can safely be considered an almost straightforward extension of the high- E_T jet phenomenon.

The UA1 Collaboration has also given the inclusive jet cross-section over the range $\sqrt{s} = 200 \div 900 \text{ GeV}$ with a nominal "jet" threshold $E_T > 5 \text{ GeV}$ and in the central region $|\eta| < 1.5$. After elaborate corrections for detection efficiency and for events leading to jets outside the acceptance they give a total jet cross-section, shown in fig.3. The cross-section is rapidly rising and it is quite large. It is instructive to compare these rates with the rate of increase of the inelastic cross-section, which we take to be $\frac{2}{3}\sigma_{tot}$ where for σ_{tot} we use the parametrization given by U.Amaldi et al.²²⁾. In the same figure we also show the experimental points [8,23,24] for the quantity $\sigma_{nsd} = \sigma_{tot} - \sigma_{el} - \sigma_{sd}$. Notice that through the energy range of interest in this paper, they all appear to fall on the curve $\frac{2}{3}\sigma_{tot}$.

To compare the above rate with QCD predictions, one can numerically integrate the 2-jet differential cross-section through the parton-parton center of mass scattering angle, i.e. write

$$\sigma_{jet}(s) = \frac{1}{2} \int dx_1 \int dx_2 \int d \cos \theta^* \frac{d\sigma}{dx_1 dx_2 d \cos \theta^*}$$

with

$$\frac{d\sigma}{dx_1 dx_2 d \cos \theta^*} = \frac{9\pi[\alpha_s(Q^2)]^2}{32s} \frac{F(x_1, Q^2)}{x_1^2} \frac{F(x_2, Q^2)}{x_2^2} \frac{(3 + \cos \theta^{*2})^3}{(1 - \cos \theta^{*2})^2}$$

where θ^* is the scattering angle in the center of mass of the parton-parton system and the integration in $\cos \theta^*$ extends between $-z_0$ and $+z_0$ with

$$z_0 = \sqrt{1 - \frac{4p_{cut}^2}{sx_1x_2}}$$

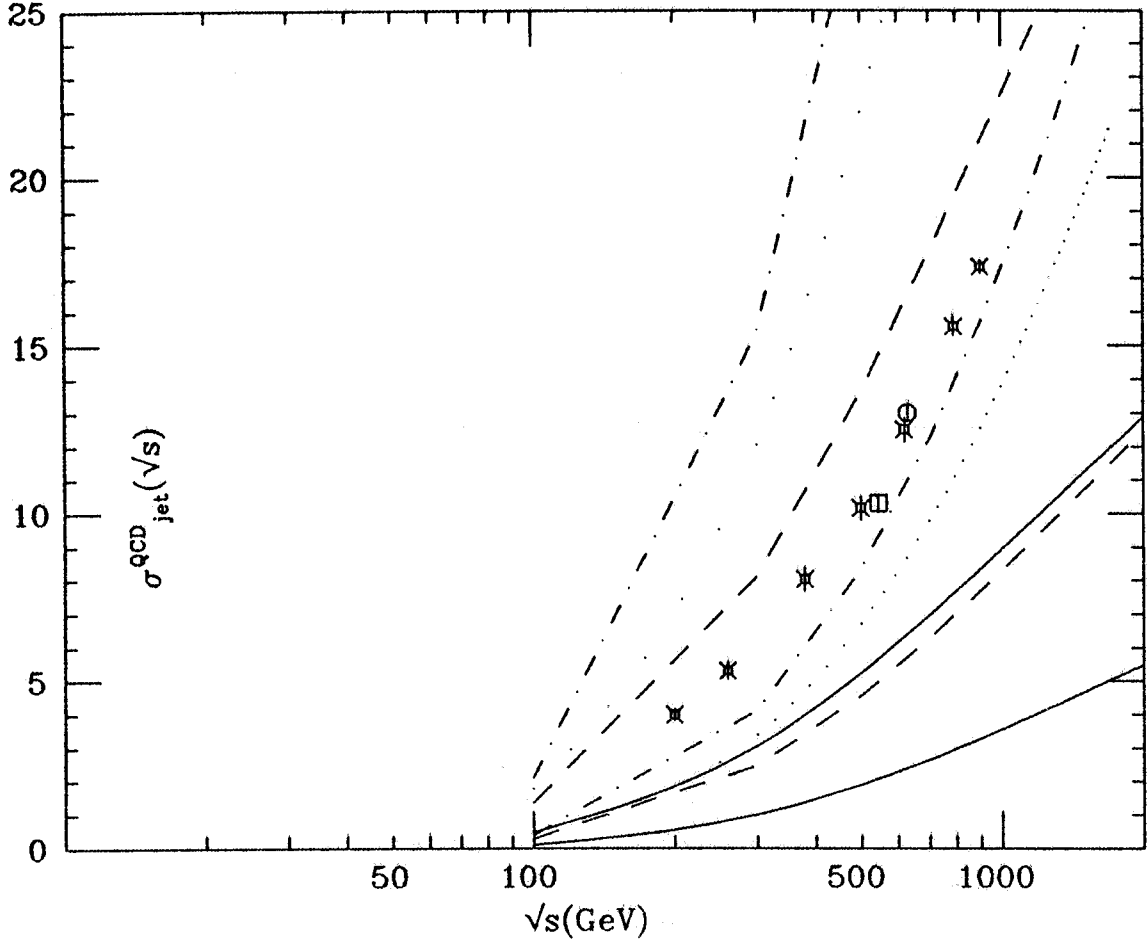


Fig.3 The inclusive mini-jet yield, $E_T^{jet} \geq 5 \text{ GeV}$, as measured by UA1, refs. (10) and (12), is compared with QCD predictions, for various values of the argument of α_s , and for the two values $p_{cut} = 3$ and 4 GeV . UA1 densities have been used for the QCD calculation. The continuous line corresponds to use $\alpha_s(sx_1x_2)$, the dashed line to $\alpha_s(\frac{x_1x_2}{16})$, dashed-dotted line to $\alpha_s(\frac{p_{cut}^2}{4})$ and the dotted line to $\alpha_s(\frac{p_T^2}{4})$.

The calculation of the jet yield is numerically simplified if one neglects the angular dependence in $\alpha_s(Q^2)$. Then the integration in $\cos\theta^*$ is straightforward and gives ^[25]

$$\int d\cos\theta^* \frac{d\sigma}{dx_1 dx_2 d\cos\theta^*} = \frac{9\pi}{16s} \frac{F(x_1, Q^2)}{x_1^2} \frac{F(x_2, Q^2)}{x_2^2} [\alpha_s(Q^2)]^2 I(p_{cut}) \quad (15a)$$

with

$$I(p_{cut}) = \frac{8sx_1x_2}{p_{cut}^2} \sqrt{1 - \frac{4p_{cut}^2}{sx_1x_2}} - 16\ln \frac{1 + \sqrt{1 - \frac{4p_{cut}^2}{sx_1x_2}}}{1 - \sqrt{1 - \frac{4p_{cut}^2}{sx_1x_2}}} + \sqrt{1 - \frac{4p_{cut}^2}{sx_1x_2}} \left(\frac{34}{3} - \frac{4}{3} \frac{p_{cut}^2}{sx_1x_2} \right) \quad (15b)$$

A further simplification is obtained if one neglects, in eq.(15), terms of higher order in $\frac{4p_{cut}^2}{sx_1x_2}$. One can then write^[26]

$$\sigma_{2-jets}(s) = \frac{9\pi}{2p_{cut}^2} \int_{\epsilon}^1 \frac{dz}{z} F\left(\frac{\epsilon}{z}, Q^2\right) \int_z^1 \frac{dx}{x} F(x, Q^2) [\alpha_s(Q^2)]^2 \quad (16)$$

with $\epsilon = \frac{4p_{cut}^2}{s}$. In order to assess how reliable this approximation is at present energies, we have compared the total 2-jet yield obtained using the complete expression, eq.(15), with the approximate form given by eq.(16) for a variety of different values for p_{cut} in the energy range $\sqrt{s} = 100 \div 1000$ GeV and found agreement within $\leq 10\%$, becoming better at higher energies.

We can now compare the size of the effect with UA1 observations. We have used UA1 parametrization for the parton densities ^[20] i.e.

$$F(x) = 6.2e^{-9.5x}$$

and we have chosen for the argument of α_s the quantity $Q^2 = \frac{p_{cut}^2}{4}$. Using the approximate expression eq.(16), one gets $\sigma = 3.52$ mb at $\sqrt{s} = 540$ GeV and for $p_{cut} = 5$ GeV, to be compared with the experimental value $\sigma = 10.3$ mb. The origin of this large disagreement has to be further investigated. We make the reasonable hypothesis that somehow the effective cut-off must be lower than the "declared" value. This may indeed be due to the presence of the underlying event which contributes more or less isotropically to the measurement of all the transverse energy deposited in the calorimeters. In our calculation we shift the energy scale by 1.5 ± 0.5 GeV relative to the value given by UA1 in order to accomodate the effects of the underlying event. Thus a jet event assigned by the UA1 algorithm to 5 GeV can be produced by the overlap of a 3.5 GeV parton together with 1.5 GeV of soft debris from the underlying event. Above considerations make evident the large degree of arbitrariness in the determination of the jet yield. There is also a strong dependence of the predictions on the assumptions on the input parameters in the QCD calculation. To this effect we have investigated several choices of densities and parameters: the "theoretical error" is quite large and that factors of order 2 can be easily accomodated

by appropriate choice of the parameters. These uncertainties in the future may be reduced by more complete calculations which would settle the question of the correct QCD scale. Present calculations indicate that values of p_{cut} in the order of a few GeV appear to saturate the experimentally observed rise of the total cross-section.

5. Beyond the Two Component Model

The previous calculations show that it is possible to interpret the second (hard) component of the total inelastic cross-section as receiving contribution from events where a hard scattering has occurred. By hard scattering we mean one where α_s is small enough to allow for a first order perturbative calculation. It should be noticed however that the quantity σ_{QCD} we have thus calculated has a very fast increase with energy due to presence of a strongly energy dependent gluon luminosity. It has been pointed out by many authors that if the probability of having a (hard) collision becomes large, then the cross section takes the form

$$\sigma_{tot} = 4\pi \int d^2\mathbf{b} \left(1 - e^{-n(\mathbf{b},s)} \right)$$

where $n(\mathbf{b},s)$ is the number of collisions at a given impact parameter and at a given center of mass energy. The quantity $n(\mathbf{b},s)$ is the one to which one can in principle apply an additive model like the two component model we described previously. Efforts in this direction have been presented at this conference [27,28] and are present in the recent literature[29]. One should notice however that different analyses give different weight to the hard component, with the result that the calculation of the total cross section relies rather heavily on the parametrization and energy dependence of the soft component. It is probably better *not* to try to describe σ_{tot} , but concentrate on the mini-jet cross-section and try to reproduce that observed jet yield. In this regard, it is still true that the calculation described in the previous section is not quite satisfactory, since it does not acknowledge the impact of the underlying event on the measured jet cross-section. In other words, even apart from the question as to whether we can calculate the rise of the total inelastic cross-section from first order QCD parton-parton scattering, we must try to develop the formalism which allows one to compare the experimental quantity measured by UA1 with the QCD predictions. Fritjof and Pythia Montecarlos appear to be moving in that direction[30]. Worth of notice in some of these efforts is the importance of the hadronic matter distribution in impact parameter space. In fact, as the authors point out, while many of the characteristic properties of the UA1 mini-jet distribution can be reproduced by the model as such, some special features seem to require a very specific b-space distribution. Thus some of the differences between models like DPM and Pythia (in the average number of collisions, for instance) can be ascribed to the different b-distributions. One must also ask as to whether it is at all possible to have an energy dependence in these distributions, not unlike what happens to the x-distribution of partons, which, as we know, has a logarithmic Q^2 dependence.

6. Conclusions

Our own assessment of the problem can be shortly summarized as follows : the contribution of hard QCD scattering is certainly important and calculable in minimum bias data at the CERN Collider energy. Predictions for the future however require further steps in the theoretical understanding of the underlying event, with particular emphasis on the hadronic matter distribution in the impact parameter space.

References

1. Z.Koba, H.B.Nielsen and P.Olesen, Nuclear Physics B40 (1972) 317.
2. G.Pancheri and Y.Srivastava, Physics Letters B 128 (1983) 433.
3. UA5 Collaboration, K.Alpgard et al., Physics Letters B 121 (1983) 209 ;
UA5 Collaboration, G.Alner et al., Physics Letters B 138 (1984) 304.
4. G.J.Alner et al., Physics Reports 154 (1987)247.
5. D.Cline, F.Halzen and J.Luthe, Physical Review Letters 31 (1973) 491;
G.Pancheri and C.Rubbia, Nuclear Physics A 418 (1984)117c.
6. UA1 Collaboration, G.Arnison et al., Physics Letters B 118 (1982)167.
7. ABCDHW Collaboration, A.Breakstone et al., Physics Letters B 132 (1983)463.
8. UA4 Collaboration, M.Bozzo et al., Physics Letters B 147 (1984)392.
9. G.Pancheri, Y.Srivastava and M.Pallotta, Physics Letters B 151 (1985) 453.
10. G.Ciapetti, Proceedings of the 5th Topical Workshop on Proton-Antiproton Collider Physics, Saint-Vincent, Aosta Valley, 25 February-1 March 1985. Ed. by M.Greco. F.Ceradini, Proceedings of the International Europhysics Conference on High Energy Physics, Bari, Italy 18-24 July 1985. Ed. by L. Nitti and G.Preparata. C.Zaccardelli, University of Rome, Italy, Thesis. 1987.
11. Chao Wei-qin, meng Ta-chung and Pan Ji-cai, Physical Review Letters 58 (1987)1399.
12. C.Albajar, Proceedings of the Workshop on Physics Simulations at high Energy, Madison 1986. Ed. by V.Barger, T.Gottschalk and F.Halzen.
13. UA5 Collaboration, G.J.Alner et al., Physics Letters B 160 (1985) 199.
14. A.Giovannini, Nuovo Cimento A 15 (1973) 543.
A.Giovannini et al., Nuovo Cimento A 24 (1974) 421.
W.J.Knox, Physical Review D 10 (1974) 65.
15. P.Carruthers and C.C.Shih, Physics Letters B 127 (1983) 242.
16. W. Thome' et al., Nuclear Physics B 129 (1977) 365.
17. J.Withmore, Physics Reports 10 C (1974) 273 ; ref. (4) fig. 4.23).
18. G.Pancheri and Y.Srivastava, Physics Letters B 159 (1985) 69.
19. R.Baltrusaitis et al., Physical Review Letters 52 (1984) 1380;
T.Hara et al., Physical Review Letters 50 (1983) 2058.

20. UA1 Collaboration, G. Arnison et al., Physics Letters B 132 (1984) 214 ; ibidem B 172 (1986)461.
21. A.Norton, These Proceedings.
22. U.Amaldi et al., Physics Letters B 66 (1977) 390.
M.Block and R.Cahn, Review of Modern Physics 57 (1985) 563.
23. R.Castaldi and G.Sanguinetti, Annual Review of Nuclear and Particle Science 35 (1985) 351.
24. M.Albrow et al., Nuclear Physics B 118 (1976) 1.
J.C.M. Armitage et al., Nuclear Physics B 194 (1982)365.
25. T.K.Gaisser and F.Halzen, Physical Review Letters 54 (1985) 1754;
G.Pancheri and Y.Srivastava, Physics Letters B 182 (1986)203.
26. A.Mueller, Proceedings of the APS/DPF Meeting (Eugene, OR, August 1985).
27. L.Durand and Hong Pi, Physical Review Letters 58 (1987) 303;
L.Durand, These Proceedings.
28. A.Capella, J.Tran Thanh Van and J.Kwiecinski, Physical Review Letters 58 (1987) 2015;
A.Capella, These Proceedings.
29. Ll.Ametller and D.Treleani, SISSA Preprint 13/87/EP. University of Trieste, 1987.
To be published in the International Journal of Modern Physics A.
30. T.Sjostrand and M.van Zijl, Physical Review D 36 (1987) 2019.
See Also Bo Andersson, These Proceedings.